

Variational Transition-State Theory Study of the Atmospheric Reaction

$\text{OH} + \text{O}_3 \rightarrow \text{HO}_2 + \text{O}_2$

LI-PING JU,¹ KE-LI HAN,¹ ANTÓNIO J. C. VARANDAS²

¹State Key Laboratory of Molecular Reaction Dynamics, Dalian Institute of Chemical Physics, Chinese Academy of Sciences, Dalian 116023, P.R. China

²Departamento de Química, Universidade de Coimbra, 3004-535 Coimbra, Portugal

Received 8 May 2006; revised 13 August 2006; accepted 10 October 2006

DOI 10.1002/kin.20226

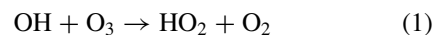
Published online in Wiley InterScience (www.interscience.wiley.com).

ABSTRACT: We report variational transition-state theory calculations for the $\text{OH} + \text{O}_3 \rightarrow \text{HO}_2 + \text{O}_2$ reaction based on the recently reported double many-body expansion potential energy surface for ground-state HO_4 [Chem Phys Lett 2000, 331, 474]. The barrier height of $1.884 \text{ kcal mol}^{-1}$ is comparable to the value of $1.77\text{--}2.0 \text{ kcal mol}^{-1}$ suggested by experimental measurements, both much smaller than the value of $2.16\text{--}5.11 \text{ kcal mol}^{-1}$ predicted by previous ab initio calculations. The calculated rate constant shows good agreement with available experimental results and a previous theoretical dynamics prediction, thus implying that the previous ab initio calculations will significantly underestimate the rate constant. Variational and tunneling effects are found to be negligible over the temperature range $100\text{--}2000 \text{ K}$. The $\text{O}_1\text{--O}_2$ bond is shown to be spectator like during the reactive process, which confirms a previous theoretical dynamics prediction. © 2007 Wiley Periodicals, Inc. Int J Chem Kinet 39: 148–153, 2007

INTRODUCTION

The last few years have witnessed great concern about the chemical composition of the Earth's atmosphere with respect to environmental issues. As a result, a number of studies have been devoted to this question [1]. One of the major topics of the recent researches

refers to the detrimental effect on the Earth's ozone layer. In particular, the reaction



is known to play an important role in the stratosphere by influencing the concentrations of many trace gases that are important to indirectly infer the concentration of hydroxyl radical. Moreover, jointly with the $\text{HO}_2 + \text{O}_3 \rightarrow \text{OH} + 2\text{O}_2$ reaction, they destroy ozone without requiring atomic oxygen, unlike similar catalytic cycles including nitrogen oxides or chlorine species [2].

Over the past few decades, both experimental and theoretical progress have been made in predicting the

Correspondence to: Ke-Li Han; e-mail: klhan@dicp.ac.cn.
Contract grant sponsor: The National Natural Science Foundation of China.

Contract grant numbers: 20373071, 20333050.
Contract grant sponsor: Fundação para a Ciência e a Tecnologia, Portugal.

Contract grant number: NSFC (20573110).
© 2007 Wiley Periodicals, Inc.

mechanism of the atmospheric reaction $\text{OH} + \text{O}_3 \rightarrow \text{HO}_2 + \text{O}_2$ [2–15]. Experimentally, the rate constant at room temperature measured by different groups [2–10] lies in the range of $(5.3\text{--}8.0) \times 10^{-14} \text{ cm}^3 \text{ molecule}^{-1} \text{ s}^{-1}$, with IUPAC [11] recommending a value of $6.7 \times 10^{-14} \text{ cm}^3 \text{ molecule}^{-1} \text{ s}^{-1}$ at 298.15 K. In addition, Anderson and Kaufman [4] measured the rate constants with a discharge flow-resonance fluorescent method over the temperature range 220–450 K, having obtained the rate coefficients expressed as $k(T) = 1.3 \times 10^{-12} \exp(-1900/RT) \text{ cm}^3 \text{ molecule}^{-1} \text{ s}^{-1}$. In turn, Ravishankara and coworkers [5] and Fischer and Davies [6] carried out rate constant measurements in both the temperature ranges 238–357 K and 223–353 K using the laser flash photolysis-resonance fluorescence technique, having obtained $k(T) = 1.82^{+0.35}_{-0.29} \times 10^{-12} \exp(-930 \pm 50/T) \text{ cm}^3 \text{ molecule}^{-1} \text{ s}^{-1}$ and $k(T) = (2.15 \pm 0.22) \times 10^{-12} \exp(-969 \pm 40/T) \text{ cm}^3 \text{ molecule}^{-1} \text{ s}^{-1}$, respectively. With a similar technique, Smith et al. [7] reported $k(T) = (1.52 \pm 0.10) \times 10^{-12} \exp(-890 \pm 60/T) \text{ cm}^3 \text{ molecule}^{-1} \text{ s}^{-1}$ in the temperature region 240–295 K. The expression of the rate constant recommended by IUPAC [11] is then $1.9 \times 10^{-12} \exp(-1000/T) \text{ cm}^3 \text{ molecule}^{-1} \text{ s}^{-1}$ for 240–450 K. Theoretically, Varandas and Zhang [12] reported the first global, partly ab initio-based, potential energy surface (PES) for ground-state HO_4 based on the double many-body expansion (DMBE) method ([16], and references therein), and used it to carry out quasi-classical trajectory (QCT) calculations of the title reaction [12–14]. The agreement for rate constants between their QCT results and the experimental data stresses the reliability of their PES. Recently, Peiró-García and Nebot-Gil [15] have presented barrier heights for the $\text{OH} + \text{O}_3 \rightarrow \text{HO}_2 + \text{O}_2$ reaction over the range 2.16–5.11 kcal mol^{-1} , depending on the level of theory employed for the ab initio electronic structure calculations. Such ab initio estimates are significantly larger than the value of 2.0 kcal mol^{-1} recommended by IUPAC [11].

The article is organized as follows. In the Methodology section, we briefly present the PES used in this work and introduce canonical variational transition-state theory (CVT). The calculated results are compared with the available data in the Results and Discussion section. The last section concludes this study.

METHODOLOGY

The present dynamical calculations are performed on the full-dimensional DMBE PES for the ground electronic state of HO_4 developed by Varandas and

Zhang in 2000 [12]. Detailed information regarding the DMBE PES is not repeated here, with the interested readers being referred to Ref. 12. Instead, we report the major characteristics of the $\text{OH} + \text{O}_3 \rightarrow \text{HO}_2 + \text{O}_2$ reaction along the minimum energy path (MEP). For this reaction, a reactants-like transition state is present and the classical barrier height is 1.056 kcal mol^{-1} . There is a shallow van der Waals well in the entrance channel whose depth is about 1.53 kcal mol^{-1} . In turn, a more stable complex is predicted in the exit channel, with its minimum lying at about 15 kcal mol^{-1} below the energy of the $\text{HO}_2 + \text{O}_2$ products.

The dynamical calculations are carried out by the CVT/SCT method developed by Truhlar and coworkers [17–22]. For a given canonical ensemble, the canonical variational rate constant for a bimolecular reaction is given by [20]

$$k^{\text{CVT}}(T) = \min_s k^{\text{GT}}(T, s) \quad (2)$$

where

$$k^{\text{GT}}(T, s) = L \frac{k_b T}{h} \frac{Q^{\text{GT}}(T, s)}{Q^{\text{R}}(T)} \exp(-V_{\text{MEP}}(s)/k_b T) \quad (3)$$

with $k^{\text{GT}}(T, s)$ being the rate constant at temperature for the generalized transition state (GTS) localized at the value of s . L is the symmetry number [23] that accounts for the reaction path multiplicity, which is equal to 2 for reaction (1). $Q^{\text{GT}}(T, s)$, and $Q^{\text{R}}(T)$ are the partition functions of the GTS and reactants, respectively. In turn, $V_{\text{MEP}}(s)$ is the classical potential energy at point s along the MEP, k_b is Boltzmann's constant, and h is the Planck constant.

To evaluate the quantum effects on the reaction-coordinate motion, one convenient way is to include a ground-state transmission coefficient $\kappa^{\text{CVT/G}}(T)$ in Eq. (2), which accounts for the tunneling and non-classical reflection effects. The quantized CVT rate constant $k^{\text{CVT/G}}(T)$ is given by

$$k^{\text{CVT/G}}(T) = \kappa^{\text{CVT/G}}(T) k^{\text{CVT}}(T) \quad (4)$$

The reaction coordinate s is the signed distance along the MEP, and the reaction path is followed using the Page-McIver method with a step size of 0.001 $(\text{amu})^{1/2} \text{ bohr}$, with a generalized normal mode analysis being performed every 0.02 $(\text{amu})^{1/2} \text{ bohr}$ along the MEP in curvilinear internal coordinates that have significantly improved the harmonic frequencies and vibrationally adiabatic ground-state (VAG) potential [24–26]. With this information, the VAG potential

in the harmonic approximation is obtained by

$$V_a^G(s) = V_{\text{MEP}}(s) + \frac{1}{2}\hbar \sum_{m=1}^{3N-7} \omega_m(s) \quad (5)$$

where $\omega_m(s)$ is the generalized normal mode frequency at a given reaction coordinate s , and the second term contains the vibrational zero-point energies (ZPEs) of all modes transverse to the reaction path. All rate constants reported here have been calculated using the POLYRATE, Version 9.1 package [27].

RESULTS AND DISCUSSION

The barrier height and heat of reaction of the $\text{OH} + \text{O}_3 \rightarrow \text{HO}_2 + \text{O}_2$ reaction are presented in Table I. As shown in this table, the classical barrier height is $1.056 \text{ kcal mol}^{-1}$ and the effective one is $1.884 \text{ kcal mol}^{-1}$ with ZPE correction included. It is noted that the value of the effective barrier height falls within the range of $1.77\text{--}2.0 \text{ kcal mol}^{-1}$ recommended by many studies [2–11]. For the heat of reaction, one gets the values of $-42.19 \text{ kcal mol}^{-1}$ (without ZPE correction) and $-41.00 \text{ kcal mol}^{-1}$ (with ZPE correction), respectively. The latter shows good agreement with the values of -43.0 and $-40.0 \text{ kcal mol}^{-1}$ suggested by Zahniser and Howard [2] and IUPAC [11], respectively. Table II compares the activation energies calculated by the CVT method with the deduced experimental data for several temperature pairs over the range $220\text{--}450 \text{ K}$. On the whole, the results obtained in this work by CVT method are slightly higher than those of the corresponding experimental values [4–7,11].

Figure 1 shows the classical potential energy curve V_{MEP} and the vibrationally adiabatic potential energy curve V_a^G together with the ZPE curve of the $\text{OH} + \text{O}_3 \rightarrow \text{HO}_2 + \text{O}_2$ reaction, where s is the reaction co-

Table I Energetics of $\text{OH} + \text{O}_3 \rightarrow \text{HO}_2 + \text{O}_2$ Reaction (Energy in kcal mol^{-1})

| Energetics | CVT | Experimental |
|-------------------------------|----------|------------------------|
| Classical barrier height | 1.056 | – |
| Effective barrier height | 1.884 | $1.77\text{--}2.0^c$ |
| Heat of reaction ^a | -42.19 | – |
| Heat of reaction ^b | -41.00 | -43.0^d -40.0^e |

^a Without ZPEs correction.

^b With ZPEs correction.

^c Experimental data [2–11].

^d Experimental data [2].

^e Experimental data [11].

Table II Activation Energies for $\text{OH} + \text{O}_3 \rightarrow \text{HO}_2 + \text{O}_2$ Reaction (Energy in kcal mol^{-1})

| T (K) | CVT | Experimental |
|---------|--------|---------------------------|
| 223–353 | 2.1923 | 1.9255 [6] |
| 238–357 | 2.2302 | 1.848 [5] |
| 240–295 | 2.1457 | 1.7685 [7] |
| 220–450 | 2.3034 | 1.9076 [4] 1.9871 [11] |

ordinate in $(\text{amu})^{1/2} \text{ bohr}$ along the MEP, with $s < 0$ and $s > 0$ indicating the reactant and product regions, respectively. All the potential curves are relative to the classical energy of the reactants. The classical and vibrationally adiabatic potential curves have similar shape and the position of the variational transition state is almost the same as that of the conventional transition state. This implies that only small variational effects are expected for this reaction, as is confirmed in the following discussion about the rate constant. In addition, the ZPE curve varies slightly with the reaction coordinate s , which suggests that the secondary kinetic isotope effect is not important for this reaction, as it has a reactants-like transition state.

The changes of bond lengths for $\text{O}_1\text{--O}_2$, $\text{O}_2\text{--O}_3$, $\text{O}_3\text{--O}_4$, and $\text{O}_4\text{--H}$ are shown in Fig. 2, where the $\text{O}_2\text{--O}_3$ and $\text{O}_3\text{--O}_4$ are the breaking and forming bonds, respectively. Clearly, the length of the $\text{O}_1\text{--O}_2$ bond is almost invariant with the reaction coordinate s , which implies that it can be regarded as a spectator during the title reaction, a finding in good agreement with the prediction of Varandas and Zhang [12] from the QCT product energy distributions. As shown in the figure, there are sharp changes in the $\text{O}_2\text{--O}_3$ and $\text{O}_3\text{--O}_4$ bond lengths around the transition-state region,

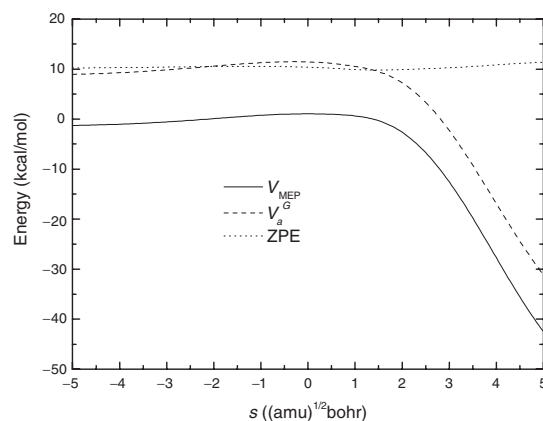


Figure 1 Potential energy curves as a function of the reaction coordinate s for the $\text{OH} + \text{O}_3 \rightarrow \text{HO}_2 + \text{O}_2$ reaction.

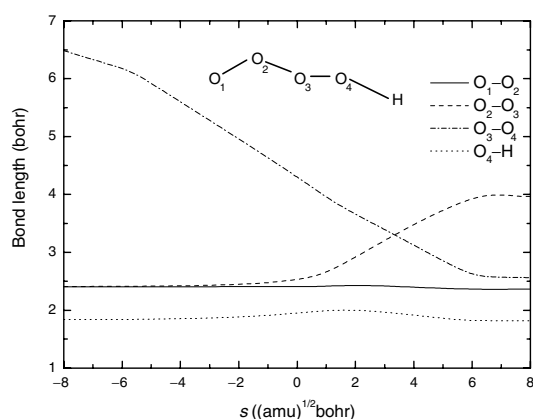


Figure 2 Bond length dependences with reaction coordinate s for the $\text{OH} + \text{O}_3 \rightarrow \text{HO}_2 + \text{O}_2$ reaction.

where the forming and breaking bonds are competing. As for the O_4H bond length, it is nearly kept constant over the entire range of the reaction coordinate s , except near the transition state. This is caused by the changes in $\text{O}_2\text{—O}_3$ and $\text{O}_3\text{—O}_4$ bonds.

In Fig. 3, the rate constants calculated by TST, CVT, and CVT/SCT methods are compared. As seen, the rate constants predicted by the above methods are in good agreement with each other, which indicates that the tunneling and variational effects do not play a significant role over the temperature range 100–2000 K. For clarity, the variational effect is quantitatively analyzed in Table III. It is noted that the location s of the variational transition state deviates from the saddle point ($s = 0$) for different temperatures. The absolute value of the deviation decreases with increasing temperature. Specifically, the absolute value of the deviation is $0.0373 (\text{amu})^{1/2} \text{ bohr}$ at $T = 2000 \text{ K}$, but $0.2463 (\text{amu})^{1/2} \text{ bohr}$ at $T = 100 \text{ K}$. The

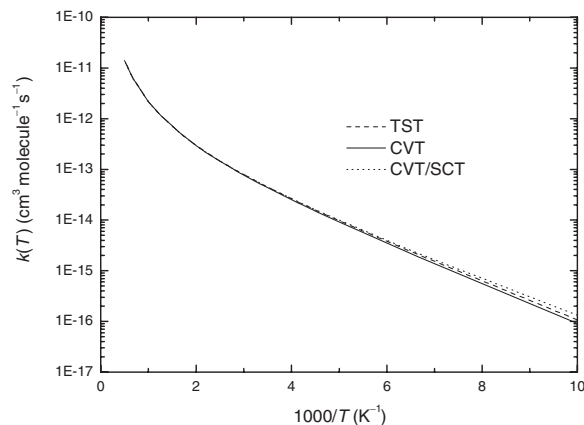


Figure 3 Comparison of the forward rate constants obtained by various TST methods for the $\text{OH} + \text{O}_3 \rightarrow \text{HO}_2 + \text{O}_2$ reaction over the temperature range 100–2000 K.

Table III Properties of Variational Transition States at Different Temperatures for the $\text{OH} + \text{O}_3 \rightarrow \text{HO}_2 + \text{O}_2$ Reaction

| T (K) | s ($(\text{amu})^{1/2}$ bohr) | V_{MEP} (kcal/mol) | V_A^G (kcal/mol) | $k_{\text{CVT}}(T)$ (cm^3 $\text{molecule}^{-1} \text{ s}^{-1}$) |
|-------------------|-------------------------------------|--------------------------------|-----------------------|--|
| S.P. ^a | 0 | 1.05587 | 11.43921 | – |
| 100 | –0.2463 | 1.03499 | 11.47902 | 9.0507E-17 |
| 150 | –0.2193 | 1.03926 | 11.47778 | 1.8732E-15 |
| 200 | –0.2027 | 1.04165 | 11.47659 | 9.1429E-15 |
| 220 | –0.1974 | 1.04238 | 11.47613 | 1.4374E-14 |
| 298 | –0.181 | 1.04451 | 11.4745 | 5.093E-14 |
| 300 | –0.1806 | 1.04456 | 11.47446 | 5.2242E-14 |
| 400 | –0.1219 | 1.05069 | 11.46649 | 1.4475E-13 |
| 450 | –0.1122 | 1.05147 | 11.4649 | 2.1235E-13 |
| 500 | –0.1045 | 1.05205 | 11.46355 | 2.955E-13 |
| 600 | –0.0923 | 1.05289 | 11.46126 | 5.1207E-13 |
| 800 | –0.0734 | 1.05398 | 11.45735 | 1.1705E-12 |
| 1000 | –0.0354 | 1.05543 | 11.44856 | 2.1723E-12 |
| 1500 | 0.0329 | 1.05549 | 11.42936 | 6.4841E-12 |
| 2000 | 0.0373 | 1.05538 | 11.42794 | 1.3935E-11 |

^a S.P. indicates the saddle point.

absolute values of $V_{\text{MEP}}(s = 0.0373) - V_{\text{MEP}}(s = 0)$ and $V_A^G(s = 0.0373) - V_A^G(s = 0)$ are 0.0005 and $0.0113 \text{ kcal mol}^{-1}$, respectively, with the corresponding ones for $V_{\text{MEP}}(s = -0.2463) - V_{\text{MEP}}(s = 0)$ and $V_A^G(s = -0.2463) - V_A^G(s = 0)$ being 0.0209 and $0.0398 \text{ kcal mol}^{-1}$, respectively. Such results confirm the small variational effect found for this reaction. The rate constants calculated in this work by the CVT method with the theoretical QCT results of Varandas and Zhang [12], and the experimental data measured by various groups [4–7,11] are plotted in Fig. 4. In general, the results predicted by CVT method are in agreement with the experimental data as well as the QCT prediction [12]. The good agreement between the present CVT and QCT results can be attributed to the prominent characteristics of $\text{OH} + \text{O}_3 \rightarrow \text{HO}_2 + \text{O}_2$ being a low barrier height ($1.056 \text{ kcal mol}^{-1}$ without ZPE correction; $1.884 \text{ kcal mol}^{-1}$ with ZPE correction) and large exothermic ($-42.19 \text{ kcal mol}^{-1}$ without ZPE correction; $-41.00 \text{ kcal mol}^{-1}$ with ZPE correction) reaction, which means that the cross-sections calculated by classical mechanics may not be sensitive to ZPE leakage. It should be added that the slight difference between the CVT and QCT results may be due to the different selected initial conditions. The former employs a thermal distribution, while the latter uses the initial-state selected conditions. Specifically, each vibrational mode in either OH or O_3 is treated thermally in the present CVT calculations, while both the OH vibration and three vibrational modes of O_3 have been fixed at their ground level in the previous QCT

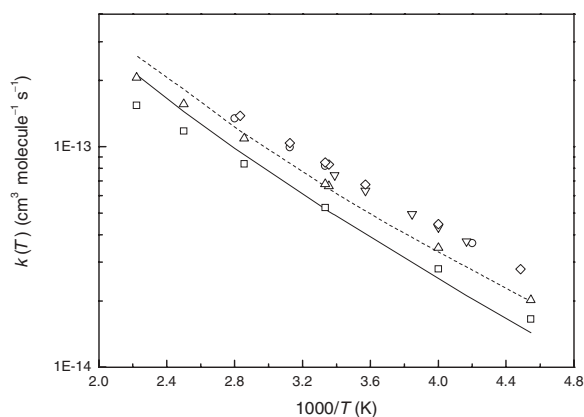


Figure 4 Comparison of the forward rate constants obtained by CVT method with previous theoretical and available experimental data for the $\text{OH} + \text{O}_3 \rightarrow \text{HO}_2 + \text{O}_2$ reaction over the temperature range 220–450 K. Solid line represents the present CVT results; dotted line, the QCT results of Ref. 12; \square , Ref. 4; \circ , Ref. 5; \triangle , Ref. 11; ∇ , Ref. 7; and \diamond , Ref. 6.

calculations [12]. In addition, the ab initio barrier height calculated in Ref. 15 for the $\text{OH} + \text{O}_3 \rightarrow \text{HO}_2 + \text{O}_2$ reaction is 2.16–5.11 kcal mol⁻¹ depending on the level of theory, which is significantly larger than the value of 1.884 kcal mol⁻¹ calculated by Varandas and Zhang [12] and 2.0 kcal mol⁻¹ recommended by IUPAC [11]. Although Peiró-García and Nebot-Gil [15] have, somewhat surprisingly, made no reference to the DMBE PES [12] in their work, we anticipate that the rate constant will be seriously underestimated at their level of ab initio theory. We conclude by focusing on the rate constant at room temperature, which is predicted by the CVT method to be 5.09×10^{-14} cm³ molecule⁻¹ s⁻¹. This is in good agreement with the results $(5.3\text{--}8.0) \times 10^{-14}$ cm³ molecule⁻¹ s⁻¹ measured by different groups [2–11].

CONCLUSIONS

We have employed CVT to systematically study the dynamical properties of the $\text{OH} + \text{O}_3 \rightarrow \text{HO}_2 + \text{O}_2$ reaction using the DMBE PES for ground-state HO_4 reported by Varandas and Zhang [12]. The calculated classical barrier height and heat of reaction are 1.056 and -42.19 kcal mol⁻¹, while the effective barrier height and heat of reaction are 1.884 and -41.00 kcal mol⁻¹. Such values are in good agreement with the barrier height of 1.77–2.0 kcal mol⁻¹ together with the heat of reaction of -40.0 and -43.0 kcal mol⁻¹ recommended experimentally [2–11]. The effective barrier height together with the corresponding experimental

data is considerably smaller than the previous ab initio results reported by Peiró-García and Nebot-Gil [15], suggesting that the rate constants predicted by them may be seriously underestimated. In fact, the rate constants calculated in this work show good agreement with both the experimental data and the QCT results of Varandas and Zhang [12]. The $\text{O}_1\text{--O}_2$ bond, which has also been shown to act as a spectator during the reactive process, is in good agreement with the QCT prediction [12]. The variational and tunneling effects have further been found to play a minor role. Finally, the agreement in energetics and thermal rate constants between our theoretical predictions and the experimental results together with the QCT calculations lends good support to the DMBE PES [12] for the title reaction.

The authors thank Professor Donald G. Truhlar for providing the POLYRATE, Version 9.1 program.

BIBLIOGRAPHY

1. Kurylo, M. J.; Orkin, V. L. *Chem Rev* 2003, 103, 5049.
2. Zahniser, M. S.; Howard, C. J. *J Chem Phys* 1980, 73, 1620.
3. Kurylo, M. J. *Chem Phys Lett* 1973, 23, 467.
4. Anderson, J. G.; Kaufman, F. *Chem Phys Lett* 1973, 19, 483.
5. Ravishankara, A. R.; Wine, P. H.; Langford, A. O. *J Chem Phys* 1979, 70, 984.
6. Fischer, S.; Davies, D. D. In Ravishankara, A. R.; Wine, P. H.; Langford, A. O. *J Chem Phys* 1979, 70, 984.
7. Smith, C. A.; Molina, L. T.; Lamb, J. J.; Molina, M. J. *Int J Chem Kinet* 1984, 16, 41.
8. Simonaitis, R.; Heicklen, J. *J Phys Chem* 1973, 77, 1932.
9. DeMore, W. B.; Tschuikow-Roux, E. *J Phys Chem* 1974, 78, 1447.
10. DeMore, W. B. *J Phys Chem* 1979, 83, 1113.
11. Atkinson, R.; Baulch, D. L.; Cox, R. A.; Hampson, R. F., Jr.; Kerr, J. A.; Troe, J. *J Phys Chem Ref Data* 1992, 21, 1125.
12. Varandas, A. J. C.; Zhang, L. *Chem Phys Lett* 2000, 331, 474.
13. Varandas, A. J. C.; Zhang, L. *Chem Phys Lett* 2001, 340, 62.
14. Zhang, L.; Varandas, A. J. C. *Phys Chem Chem Phys* 2001, 3, 1439.
15. Peiró-García, J.; Nebot-Gil, L. *Chem Phys Chem* 2003, 4, 843.
16. Varandas, A. J. C. In *Conical Intersections: Electronic Structure, Dynamics and Spectroscopy*; Yarkony, D.; Koppel, H.; Domcke, W. (Eds.); World Scientific Publishing: Singapore; 2004; Ch. 5.
17. Skodje, R. T.; Truhlar, D. G.; Garrett, B. C. *J Phys Chem* 1981, 85, 3019.

18. Truhlar, D. G.; Isaacson, A. D.; Skodje, R. T.; Garrett, B. C. *J Phys Chem* 1982, 86, 2252.
19. Truhlar, D. G.; Garrett, B. C. *Annu Rev Phys Chem* 1984, 35, 159.
20. Truhlar, D. G.; Isaacson, A. D.; Garrett, B. C. In *Theory of Chemical Reaction Dynamics*; Baer, M. (Ed.), Chemical Rubber: Boca Raton, FL; 1985.
21. Truhlar, D. G.; Garrett, B. C. *J Chem Phys* 1987, 84, 365.
22. Liu, Y.-P.; Lynch, G. C.; Truong, T. N.; Lu, D.-h.; Truhlar, D. G. *J Am Chem Soc* 1993, 115, 2408.
23. Pollak, E.; Pechukas, P. *J Am Chem Soc* 1978, 100, 2984.
24. Jackels, C. F.; Gu, Z.; Truhlar, D. G. *J Chem Phys* 1995, 102, 3188.
25. Nguyen, K. A.; Jackels, C. F.; Truhlar, D. G. *J Chem Phys* 1996, 104, 6491.
26. Chuang, Y.-Y.; Truhlar, D. G. *J Chem Phys* 1997, 107, 83.
27. Corchado, J. C.; Chuang, Y.-Y.; Fast, P. L.; Villà, J.; Hu, W.-P.; Liu, Y.-P.; Lynch, G. C.; Nguyen, K. A.; Jackels, C. F.; Melissas, V. S.; Lynch, B. J.; Rossi, I.; Coitiño, E. L.; Fernandez-Ramos, A.; Pu, J. Z.; Albu, T. V.; Steckler, R.; Garrett, B. C.; Isaacson, A. D.; Truhlar, D. G. POLYRATE, Version 9.1; University of Minnesota: Minneapolis; 2002.